

DBR tapered diode laser with 12.7 W output power and nearly diffraction-limited, narrowband emission at 1030 nm

André Müller¹ · Jörg Fricke¹ · Frank Bugge¹ · Olaf Brox¹ · Götz Erbert¹ · Bernd Sumpf¹

Received: 17 November 2015 / Accepted: 6 February 2016 / Published online: 6 April 2016
© Springer-Verlag Berlin Heidelberg 2016

Abstract A 1030 nm distributed Bragg reflector (DBR) tapered diode laser with nearly diffraction-limited emission is presented. The laser provides an optical output power of 12.7 W with an electro-optical efficiency >40 %. At 10.5 W of optical output power, a central lobe power content of 8.1 W and a nearly diffraction-limited beam propagation ratio of $M^2 = 1.1$ ($1/e^2$) are obtained. The corresponding brightness is $700 \text{ MW cm}^{-2} \text{ sr}^{-1}$. Compared to previous approaches, intrinsic wavelength stabilization is obtained by a third-order DBR grating manufactured using more reproducible electron-beam lithography. A narrowband emission is measured over the whole power range with a spectral bandwidth of about 17 pm at 12.5 W. Based on the measured electro-optical, spectral and spatial properties, the laser is suitable for applications requiring narrowband, high-power emission with high spatial quality.

1 Introduction

Near-infrared diode lasers providing high optical output power with good spatial beam quality and narrowband emission are required for many different applications. For example, nonlinear frequency conversion of such lasers into the visible spectral range enables new applications currently not addressed by direct emitting diode lasers.

Diode lasers suitable for high-power nonlinear frequency conversion should ideally provide several watts

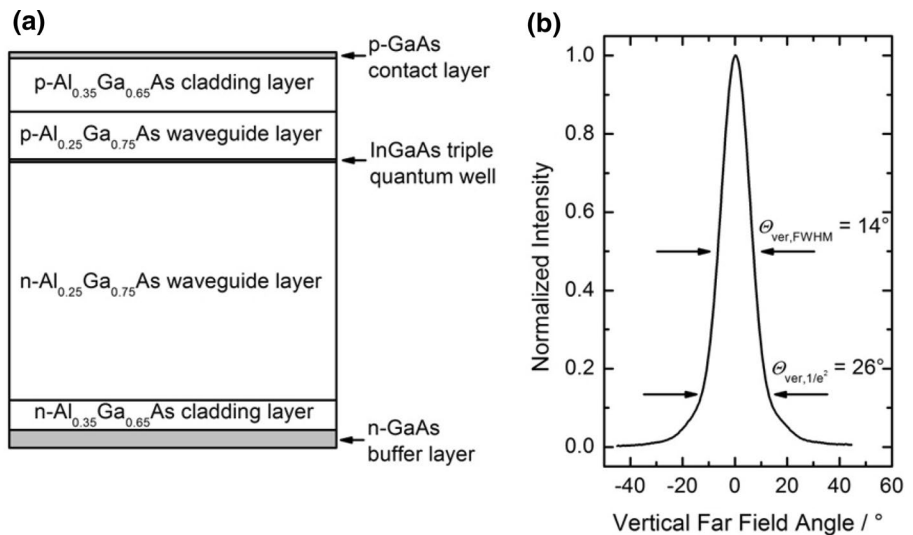
of near-diffraction-limited emission and spectral bandwidths below the acceptance bandwidths of the corresponding nonlinear crystals [1, 2], typically smaller than 100 pm. High-power near-diffraction-limited emission can be obtained with tapered diode lasers. Here, the emission of a ridge waveguide (RW) is monolithically coupled to a tapered section, acting as a power amplifier [3, 4]. The angle of the gain-guided amplifier is adapted to the diffraction of the emission leaving the RW. This results in power amplification while the lateral single-mode profile provided by the RW is maintained. Narrowband emission is obtained by an additional wavelength selective feedback [5, 6], e.g., by implementing intrinsic DBR gratings inside the RW. With such a DBR tapered diode laser, up to 8 W of nearly diffraction-limited output power with narrowband emission at 1060 nm was demonstrated [7]. By single-pass frequency doubling, 1.5 W was generated at 530 nm [8], enabling these diode lasers to be applied as pump sources of titanium:sapphire lasers [9].

In comparison with tapered diode lasers, the implemented gratings in DBR tapered diode lasers also serve as additional mode filters, enhancing the spatial beam quality [10]. Due to the DBR gratings, the rear facets can be anti-reflection coated. Therefore, only light guided within the single-mode ridge waveguide is reflected by the grating and coupled back to the tapered section for amplification. Consequently, high-quality gratings with high diffraction efficiencies are crucial in order to obtain narrowband, near-diffraction-limited emission. For previous devices discussed in [7], the intrinsic wavelength stabilization was obtained by sixth-order DBR gratings [11]. The gratings and RWs for the lasers were defined and formed simultaneously, using i-line wafer stepper lithography and reactive ion etching, respectively. Therefore, a trade-off had to be made regarding the optimization of gratings and

✉ André Müller
andre.mueller@fbh-berlin.de

¹ Ferdinand-Braun-Institut, Leibniz-Institut für Höchstfrequenztechnik, Gustav-Kirchhoff-Str. 4, 12489 Berlin, Germany

Fig. 1 **a** Developed *vertical layer* structure for the presented 1030 nm diode laser. The structure is based on a TQW in a 4.8 μm asymmetric super large optical cavity. **b** Normalized intensity distribution of the *vertical far field* for the developed layer structure



waveguides. In addition, obtaining high reflectivities with high-order gratings requires high duty cycles. In practice, the latter are achieved by v-shaped feature dimensions at the expense of reproducibility. In comparison with i-line wafer stepper lithography, the increased resolution of electron-beam lithography helps to realize structures with significantly smaller dimensions, i.e., the implementation of low-order gratings with increased diffraction efficiencies. The gratings have more controllable feature dimensions and are realized independently from the RW. Regarding the obtained reflectivities, electron-beam lithography therefore becomes more reproducible and the manufacturing process is much more flexible.

In this paper, we present our results for a 1030 nm tapered diode laser with an intrinsic third-order DBR grating realized by electron-beam lithography. First, the vertical structure and corresponding material parameters are discussed. Afterward, the lateral layout, facet coating and mounting of the laser are briefly described. Finally, the results regarding electro-optical, spectral and spatial properties of the laser are provided.

2 Vertical layer structure and material characterization

The vertical layer structure developed for this 1030 nm diode laser is shown in Fig. 1a. The structure is grown by metal–organic vapor phase epitaxy and is based on an InGaAs triple quantum well (TQW). The TQW is positioned in a 4.8- μm -wide asymmetric super large optical cavity [12]. The thick waveguide with respect to the thickness of the active region results in a low vertical far-field angle of $\theta_{\text{ver,FWHM}} = 14^\circ$, shown in Fig. 1b. A TQW is selected in order to compensate the reduced vertical

Table 1 Material data of the developed structure for 1030 nm diode lasers

λ (nm)	I_{th} (mA)	S (W/A)	η_d	T_0 (K)	$\theta_{\text{ver,FWHM}}$ ($^\circ$)
1029	315	0.56	0.93	173	14

confinement, i.e., a reduced overlap of the optical field with the active region, related to the super large optical cavity. The asymmetric position of the active region within the optical cavity, here a ratio of 20:80 is realized, allows for an enhanced spatial beam quality [13].

In order to determine the quality of the developed structure, electro-optical and spectral characteristics are measured for an uncoated, unmounted broad area device with 100 μm stripe width and 1 mm length. The measurements are taken in pulsed mode (5 kHz, 1 μs). The measured emission wavelength λ , the threshold injection current I_{th} , the slope efficiency S , the differential efficiency η_d , the characteristic temperature of the threshold current T_0 and the vertical far-field angle θ_{ver} are summarized in Table 1.

The measured emission wavelength matches the anticipated spectral range and will slightly shift to longer wavelengths at CW operation. Laser operation starts at 315 mA. The device provides a high slope efficiency and differential efficiency of 0.56 W/A and 93 %, respectively. A characteristic temperature of 173 K indicates a good temperature insensitivity of the threshold current. The low vertical far field of 14° enables easy beam shaping.

In order to determine the transparency current density, the modal gain coefficient, the internal efficiency and the internal losses, measurements of electro-optical and spectral characteristics are also taken for devices with different resonator lengths. From measurements of the threshold current density as a function of the inverse cavity length,

a transparency current density of $j_{tr} = 173 \text{ A/cm}^2$ and a modal gain coefficient of $\Gamma g_0 = 19 \text{ cm}^{-1}$ are calculated. From measurements of the slope efficiency as a function of the cavity length, a high internal efficiency of $\eta_i \approx 1.0$ and low internal losses of $\alpha_i = 1.5 \text{ cm}^{-1}$ are obtained. Altogether, the discussed parameters indicate the high quality of the laser material, suitable for the processing of 1030 nm DBR tapered diode lasers.

3 Lateral layout, facet coating and mounting of the 1030 nm DBR tapered diode laser

A scheme of the tapered diode laser presented in this paper is shown in Fig. 2. The laser consists of three sections, namely a 1-mm-long DBR grating, a 1 mm RW and a 4 mm tapered amplifier (TA). The ridge waveguide width and the full tapered angle are $5 \mu\text{m}$ and 6° , respectively.

Compared to previous approaches [7, 16], the intrinsic DBR grating is a third-order grating realized by electron-beam lithography. The grating period is about 460 nm. The grating is etched through the p-side of the vertical structure

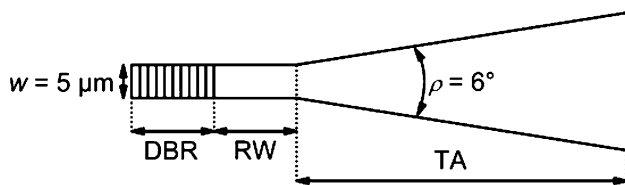


Fig. 2 Lateral layout of the presented 1030 nm DBR tapered diode laser

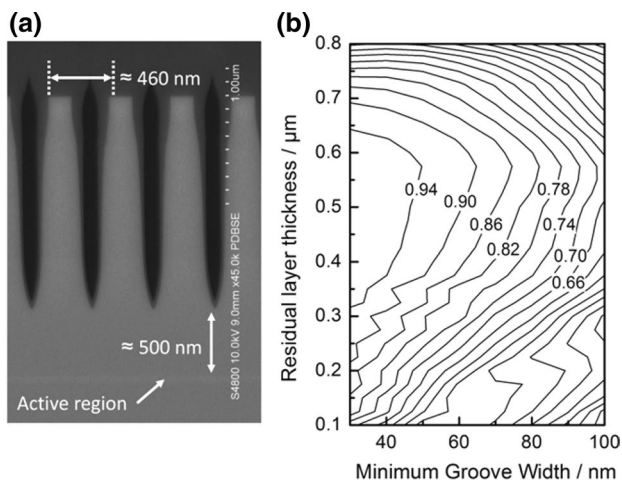


Fig. 3 **a** Scanning electron microscope image showing parts of a DBR grating manufactured by electron-beam lithography for the presented 1030 nm laser. **b** Numerical simulations of the diffraction efficiency as a function of the minimum groove width and the residual layer thickness. Solid lines indicate constant diffraction efficiencies

with a residual layer thickness to the active region of about 500 nm. The corresponding scanning electron microscope image in Fig. 3a shows consistent grating grooves and residual layer thicknesses. In Fig. 3b, numerical simulations of the diffraction efficiency as a function of minimum groove width and residual layer thickness are shown. The simulations are based on the CAvity Modelling FRamework tool (CAMFR, <http://camfr.sourceforge.net/>). For the third-order grating, a maximum diffraction efficiency of 94 % is calculated. Following the realization of the grating, the RW of the DBR tapered diode lasers is processed by reactive ion etching. The layout of the gain-guided tapered amplifier is defined by shallow ion implantation.

The facets of the device are anti-reflection coated including a facet passivation process on both sides [14]. The measured reflectivities are $R_F = 0.4 \%$ on the front facet and $R_R < 8 \times 10^{-4}$ on the rear facet. The latter helps to suppress contributions of unwanted lateral higher-order modes propagating outside the RW [10]. The laser is mounted p-side up on a copper tungsten heat spreader on a conduction cooled package mount with a footprint of $25 \text{ mm} \times 25 \text{ mm}$. The RW and the TA can be controlled independently, which enables slight influences on the spatial quality of tapered lasers [15].

4 Electro-optical, spectral and spatial characteristics

For all measurements, the 1030 nm DBR tapered diode laser is mounted on a Peltier-cooled heat sink, stabilized at a temperature of 15°C . The laser is operated in CW mode with a constant injection current to the RW of 300 mA. Figure 4a shows the power–voltage–current characteristics. The voltage and optical output power are measured as a function of the injection current to the TA, increased in 100 mA steps. The voltage is measured at the TA using a digital multimeter (2000/E, Keithley). The optical output power is measured with a power detector positioned in front of the laser into the diverging beam (UP19 K-15S-H5-DO, Gentec Electro-Optics).

The device starts to lase at about 2 A to the TA. The optical output power increases linearly until an injection current of about 13 A ($P \approx 9.1 \text{ W}$). The measured slope efficiency is 0.83 W/A. At higher injection currents, the onset of a roll-over is observed and the slope efficiency decreases. Between 16 and 20 A, a slope efficiency of 0.37 W/A is measured. At an injection current of 20 A, the optical output power is 12.7 W. By a linear extrapolation of the measured voltage through the y-axis, a diode voltage of 1.3 V and a differential resistance of 14 mΩ are obtained. The latter indicates low electric losses for the device and the applied mounting technology. The electro-optical

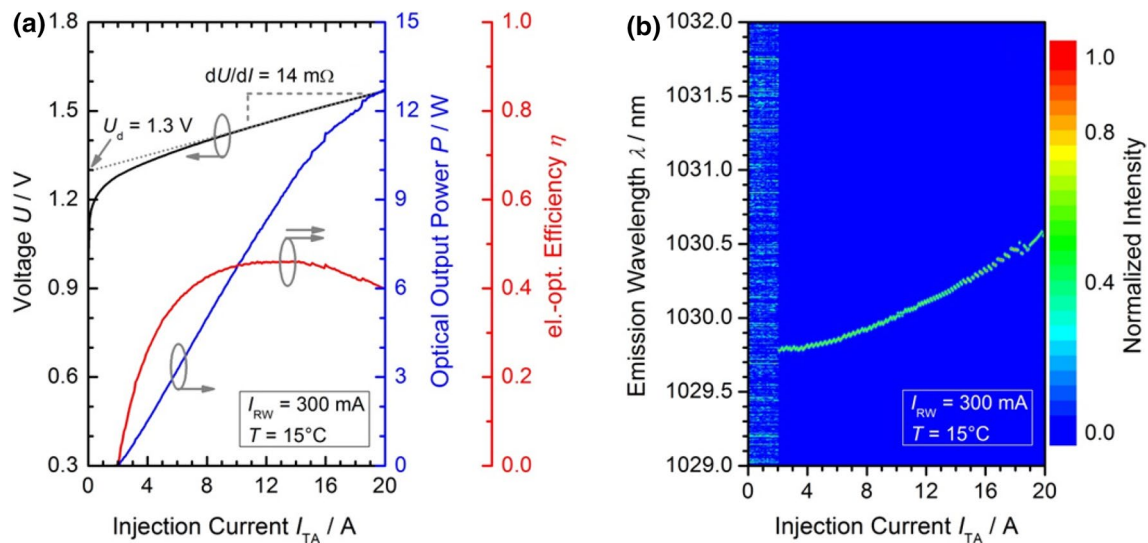


Fig. 4 **a** Voltage, optical output power and electro-optical efficiency measured as a function of the injection current to the tapered amplifier of the 1030 nm DBR tapered diode laser. **b** Corresponding emission spectra as a function of the injection current

efficiency is calculated considering the power–voltage–current characteristics and the electrical power applied to the RW ($I_{RW} = 300 \text{ mA}$, $U_{RW} = 1.8 \text{ V}$). The maximum electro-optical efficiency is 46 % at an optical output power of 9.1 W. Despite the onset of a roll-over, an efficiency of 40 % is still measured at 12.7 W of optical output power.

Figure 4b shows a plot of the corresponding emission spectra measured as a function of the injection current to the TA. All spectra are individually normalized in intensity to 1. The spectra are measured using a double echelle monochromator with a spectral resolution of 10 pm at emission wavelengths of 1030 nm (Demon, LTB Lasertechnik Berlin). The plot shows narrowband emission over the whole power range. The temperature-related wavelength shift is about 0.1 nm/A. In conjunction with the observed temperature tuning, mode hops with a spectral distance of about 20 pm are measured. This distance corresponds to the expected free spectral range of the 6-mm-long DBR tapered diode laser. The observed increase in mode hopping at injection currents $>16 \text{ A}$ is potentially caused by the impact of the related temperature rise within the device. The latter also becomes apparent in a reduction in the electro-optical efficiency and the course of the power–current characteristics. The tuning and the mode hops result in an overall wavelength shift of about 0.8 nm between laser threshold and maximum injection current. The peak wavelength is at around 1030.2 nm within a spectral window of $\pm 0.4 \text{ nm}$.

Figure 5 shows a single emission spectrum measured at 12.5 W of output power with a peak wavelength of 1030.50 nm. With a measured spectral width of 17 pm (FWHM), limited by the resolution of the spectrum

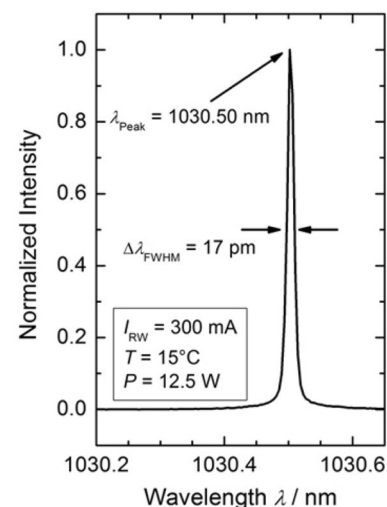


Fig. 5 Normalized emission spectrum at 12.5 W optical output power

analyzer, the diode laser is suitable for nonlinear frequency conversion.

The lateral spatial characteristics of the diode laser are obtained from measurements according to the method of the moving slit (ISO Standard 11146). Figure 6 shows the normalized intensity distributions of the beam waist (a), far field (b) and near field (c), measured at 10.5 W of output power. The measured beam waist width is $6 \mu\text{m}$ ($1/e^2$). The central lobe contains 77 % of the measured intensity; i.e., a power content of $P_{CL} = 8.1 \text{ W}$ is obtained. The difference of 2.4 W compared to the optical output power is contained in side lobes next to the central lobe. The obtained central

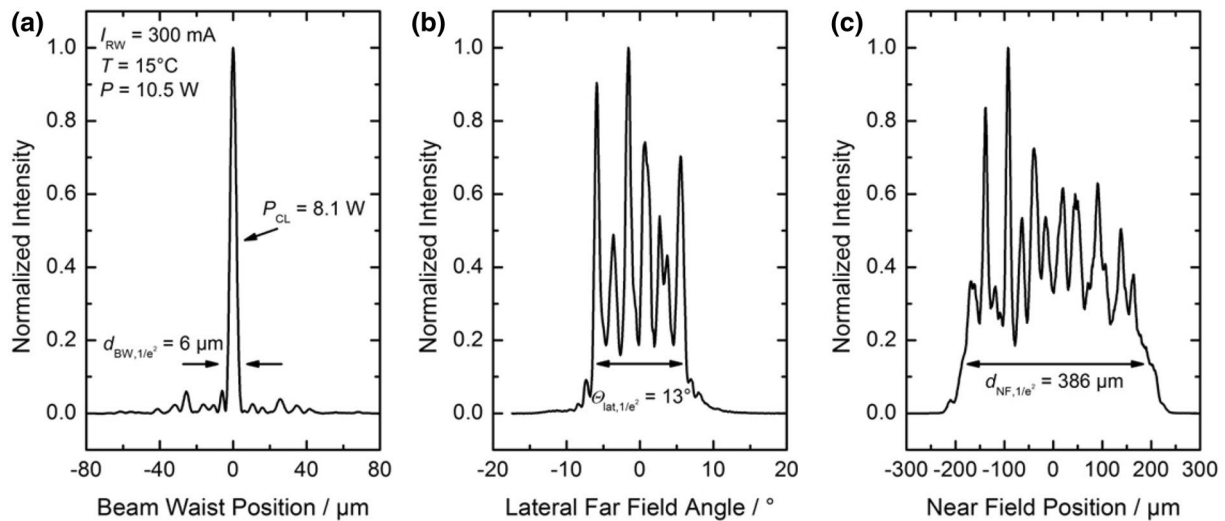


Fig. 6 Normalized intensity distributions of the beam waist (a), lateral far field (b) and near field (c), measured at 10.5 W of optical output power

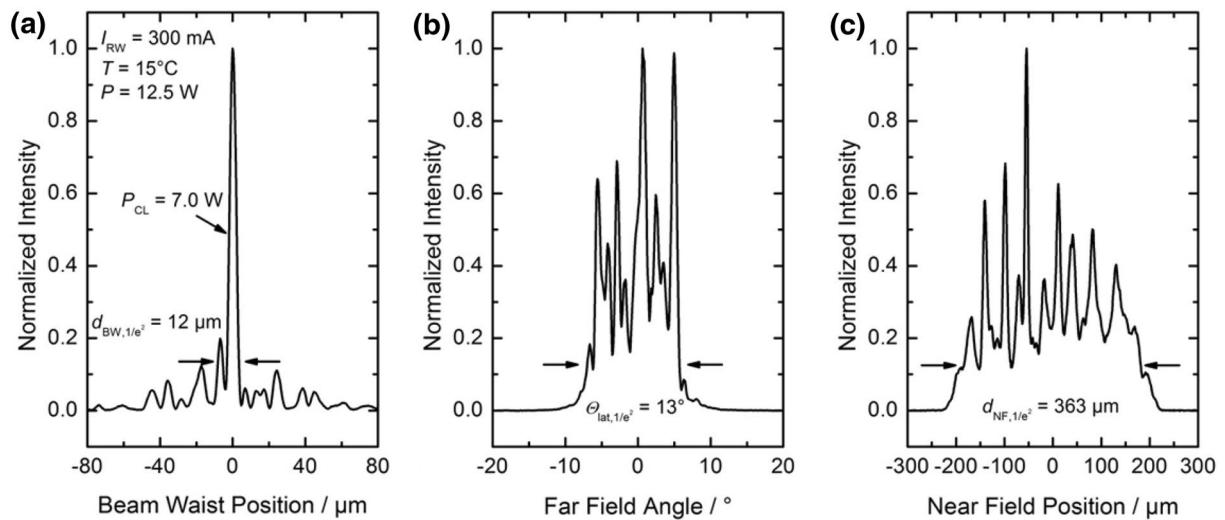


Fig. 7 Normalized intensity distributions of the beam waist (a), lateral far field (b) and near field (c), measured at 12.5 W of optical output power

lobe power content is comparable to previous results [7, 16]. The measured lateral far-field angle is 13° ($1/e^2$). A beam propagation ratio of $M^2 = 1.1$ ($1/e^2$) is calculated from the beam waist width and lateral far-field angle, indicating nearly diffraction-limited emission. The brightness calculated for the central lobe is $B \approx 700 \text{ MW cm}^{-2} \text{ sr}^{-1}$. The measured near-field width of $386 \mu\text{m}$ ($1/e^2$) is close to the calculated width for a 4-mm-long, 6° tapered amplifier. For applications involving tapered lasers, the astigmatism, i.e., the longitudinal distance of the beam waist with respect to the front facet of the laser, is an important parameter. The measured astigmatism at 10.5 W of output power is 1.54 mm.

The beam propagation ratio is also measured at 12.5 W (Fig. 7). Here, minor changes in the shape and width of the far-field and near-field intensity distributions are observed. The measured far-field angle is still 13° ($1/e^2$). The near-field intensity distribution is slightly more modulated, and the measured width is $363 \mu\text{m}$ ($1/e^2$). The beam waist intensity distribution shows an increased number of distinct side lobes causing a significant reduction in the central lobe power content to $P_{\text{CL}} = 7 \text{ W}$. The measured beam waist width is about $12 \mu\text{m}$ ($1/e^2$), resulting in a beam propagation ratio of $M^2 = 1.9$ ($1/e^2$). Such degradations at higher output powers have been previously observed for tapered lasers [16]. Therefore, a trade-off between the total optical

output power and the central lobe power content has to be made. The measured astigmatism at 12.5 W of output power is 1.64 mm.

5 Summary

A 1030 nm DBR tapered diode laser providing 12.7 W of optical output power and an electro-optical efficiency >40 % is presented. For intrinsic wavelength stabilization, a third-order DBR grating is manufactured by electron-beam lithography. Narrowband emission is obtained over the whole power range, and a spectral width of 17 pm is measured at 12.5 W. Applying electron-beam lithography for intrinsic wavelength stabilization is therefore suitable for manufacturing DBR tapered diode lasers. At 10.5 W of optical output power, nearly diffraction-limited beam quality with a beam propagation ratio of $M^2 = 1.1$ ($1/e^2$) and a central lobe power content of 8.1 W are obtained. The measured brightness is $700 \text{ MW cm}^{-2} \text{ sr}^{-1}$. Based on the measured electro-optical, spectral and spatial properties, the laser is suitable for applications such as nonlinear frequency conversion requiring narrowband, high-power emission with high spatial quality.

Acknowledgments The authors acknowledge financial support from the European Union project FAMOS (Seventh Framework Program, Information and Communication Technologies, Contract 317744).

References

1. R.W. Boyd, *Nonlinear Optics*, 2nd edn. (Academic Press, San Diego, London, 2003)
2. W.P. Risk, T.R. Gosnell, A.V. Nurmikko, *Compact Blue-Green Lasers* (Cambridge University Press, Cambridge, 2003)
3. J.N. Walpole, *Opt. Quantum Electron.* **28**, 623 (1996)
4. E.S. Kintzer, J.N. Walpole, S.R. Chinn, C.A. Wang, L.J. Missaggia, *IEEE Photon. Technol. Lett.* **5**, 605 (1993)
5. G.V. Agrawal, N.K. Dutta, *Semiconductor Lasers*, 2nd edn. (Kluwer Academic Publishers, Dordrecht, 1993)
6. J. Buus, M.-C. Amann, D.J. Blumenthal, *Tunable Laser Diodes and Related Optical Sources* (Wiley-Intersciences, Hoboken, 2005)
7. B. Sumpf, K.H. Hasler, P. Adamiec, F. Bugge, F. Dittmar, J. Fricke, H. Wenzel, M. Zorn, G. Erbert, G. Tränkle, *IEEE J. Sel. Top. Quantum Electron.* **15**, 1009 (2009)
8. O.B. Jensen, P.E. Andersen, B. Sumpf, K.-H. Hasler, G. Erbert, P.M. Petersen, *Opt. Express* **17**, 6532 (2009)
9. A. Müller, O.B. Jensen, A. Unterhuber, T. Le, A. Stingl, K.-H. Hasler, B. Sumpf, G. Erbert, P.E. Andersen, P.M. Petersen, *Opt. Express* **19**, 12156 (2011)
10. S.N. Kaunga-Nyirenda, S. Bull, J.J. Lim, K.-H. Hasler, J. Fricke, E.C. Larkins, *IET Optoelectron.* **8**, 99 (2013)
11. J. Fricke, H. Wenzel, M. Matalla, A. Klehr, G. Erbert, *Semicond. Sci. Technol.* **20**, 1149 (2005)
12. A. Knauer, G. Erbert, R. Staske, B. Sumpf, H. Wenzel, M. Weyers, *Semicond. Sci. Technol.* **20**, 621 (2005)
13. J.M.G. Tijero, H. Odriozola, L. Borruel, I. Esquivias, S. Sujecki, E.C. Larkins, *IEEE Photon. Technol. Lett.* **19**, 1640 (2007)
14. P. Ressel, G. Erbert, U. Zeimer, K. Häusler, G. Beister, B. Sumpf, A. Klehr, G. Tränkle, *IEEE Photon. Technol. Lett.* **17**, 962 (2005)
15. H. Odriozola, J.M.G. Tijero, L. Borruel, I. Esquivias, H. Wenzel, F. Dittmar, K. Paschke, B. Sumpf, G. Erbert, *IEEE J. Quantum Electron.* **45**, 42 (2009)
16. C. Fiebig, G. Blume, M. Übernickel, D. Feise, C. Kaspari, K. Paschke, J. Fricke, H. Wenzel, G. Erbert, *IEEE J. Sel. Top. Quantum Electron.* **15**, 978 (2009)